



Original Research Article

Continuous flow injection analysis via NAG-4SX3-3D analyzer utilized to determination of resorcinol

Nagham Shakir Turkie, Sarah Faris Hameed *

Department of chemistry, College of science, University of Baghdad, Baghdad, Iraq

ARTICLE INFORMATION

Received: 11 February 2022
Received in revised: 26 April 2022
Accepted: 1 May 2022
Available online: 15 May 2022

DOI: 10.22034/ajgc.2022.2.3

KEYWORDS

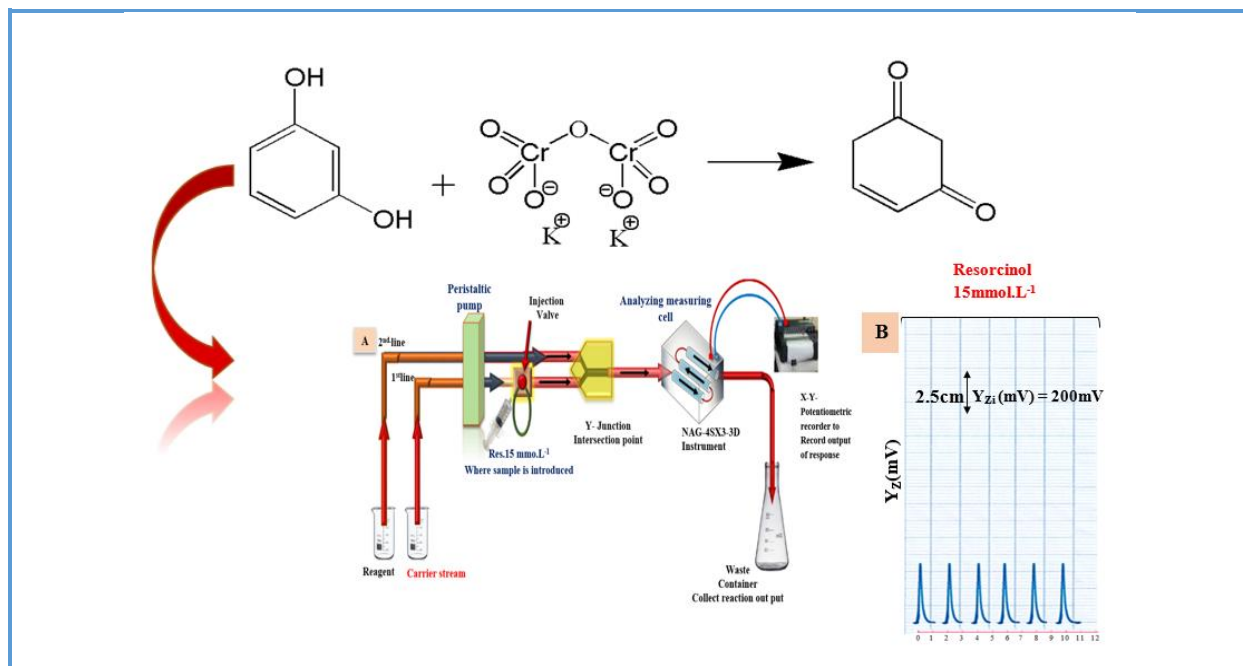
Resorcinol
Continuous flow injection analysis
Turbidity
Potassium dichromate

ABSTRACT

A fast and sensitive method for detecting resorcinol by producing yellowish-green color species using the reaction of potassium dichromate with resorcinol in a sulfuric acid medium. NAG-4SX3-3D analyzer was used to evaluate the transducer energy response. To improve the sensitivity of the newly developed approach, the relevant parameter was explored. The linear range (0.05-32) mmol.L⁻¹ for resorcinol measurement and RSD percent for the repetition (n=6) was significantly lower than 0.3% for (0.7, 23 millimol.L⁻¹) with L.O.D.=48.1687 ng/sample from the progressive dilution across the calibration graph's lowest concentration linear dynamic range (r=0.9997), (correlation coefficient), percentage linearity (R² %=99.95). The proposed approach was compared to the previous technique (UV-spectrophotometric at λ_{\max} =273 nm). It can be concluded that, in addition to the technique's sensitivity (developed) and the use of a few chemicals, it outperforms the 10 mm irradiation of the classic reference method. Furthermore, continual dilution in CFIA enables the handling of high or low concentrations, opening up a larger range of applications. Based on the foregoing, the developed methodology is judged to be the most suited for resorcinol molecules compared to the reference techniques.

© 2022 by SPC (Sami Publishing Company), Asian Journal of Green Chemistry, Reproduction is permitted for noncommercial purposes.

Graphical Abstract



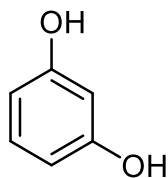
Introduction

Resorcinol (Res) 1,3-isomer of benzenediols, as illustrated in Scheme 1, is a dihydric phenol exhibiting characteristic phenol reactivity. It is a monoaromatic compound having two hydroxyl groups in meta position to each other that may be found in fossil fuels in the heartwood of *Artocarpus* and *Moraceae* species. Resorcinol ring-containing components have been discovered in various natural compounds, including plant phenolics which include resorcinol ring-containing components and are widely distributed in nature [1]. Resorcinol has widely utilized in various industries, including the production of rubber products [2]. Resorcinol is used in the rubber industry as a primer in latex fabric coating [3] and as a glue in rubber product manufacture, such as when attaching the ends of a conveyor belt. It is included in many hair color products because of its unique functioning as a coupler. It is also found in medicinal items [4] such as eye drops

that can be purchased without a prescription and a variety of ointments for disorders as psoriasis and acne.

Local hyperemia, corrosion, itching, dermatitis, and the loss of superficial layers of the skin may occur when solutions or salves containing 3 to 25% resorcinol are used [5]. It causes skin and eye discomfort if eaten, absorbed, or breathed through the skin. The drug may have effects on the blood, inducing methaemoglobin production. It is considered goitrogenic, causing hypothyroidism. Resorcinol was discovered in an aqueous solution [6] as an intermediary in the anaerobic decomposition of methoxyphenol and as an irradiation product of 3-chlorophenol.

There are many methods for the determination of resorcinol, such as electromagnetic sensor [7], electrochemical activation of graphene sheets embedded in carbon films [8], and a surfactant enhanced graphene paste electrode [9], electrochemical oxidation [10], electrochemical detection [11].



Scheme 1. Structure of resorcinol

Experimental

Materials and methods

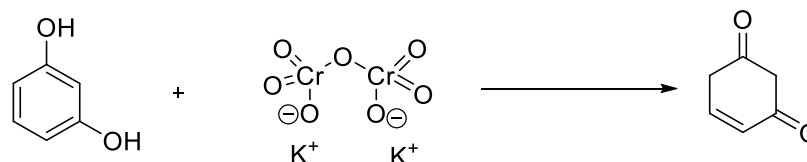
The solutions were produced using distilled water, and all of the compounds used were analytical reagent grade. By dissolving 11 g in 500 mL of distilled water, a 0.2 M standard solution of Resorcinol $C_6H_4(OH)_2$ with molecular weight $110.1 \text{ g}\cdot\text{mol}^{-1}$, BDH was made. A standard solution of potassium dichromate $K_2Cr_2O_7$ with a molecular weight of $294.22 \text{ g}\cdot\text{mol}^{-1}$ Hopkin and Williams LTD was made by dissolving 18.38 g of potassium dichromate in 250 mL of distilled water.

Apparatus

A flow cell manufactured from a handmade NAG-4SX3-3D analyzer [12] was used to obtain the output from the attenuation of incident light (0–180°). Figure 1a Potentiometric recorders were used to record the output signals (Siemens, Germany). A six-port injection valve and an ismastic peristaltic pump with a sample loop (Teflon, variable length), the traditional procedures were carried out using a Uv-spectrophotometric (Shimadzu, Japan).

Methodology

A manifold design for determining an aromatic organic chemical (resorcinol) Figure 1a by forming colored species with potassium dichromate. It consists of a two-line manifold system attached to the NAG-4SX3-3D analyzer. A sample segment introduction unit (injection valve with load injection location) is included in the system, allowing a certain quantity to be injected repeatedly with flawless dependability. The first line provides distilled water as a carrier stream for the sample zones of resorcinol $15 \text{ mmol}\cdot\text{L}^{-1}$ with $115 \text{ }\mu\text{L}$ as a sample volume to meet with potassium dichromate in the second line at a $2.8 \text{ mL}\cdot\text{min}^{-1}$ flow rate for each line by Y-junction point before being introduced to the NAG-4SX3-3D analyzer. The x-t potentiometric record output was used to quantify the transducer energy response for the attenuation of incident light on colored species for a yellowish-green species which formed. Each solution was investigated three times. Scheme 2 proposed a mechanism for the oxidation of resorcinol by potassium dichromate. Figure 2 displays the output Y_z (mV) vs. t_{\min} (d_{mm}) of the NAG-4SX3-3D analyzer transducer for $15 \text{ mmol}\cdot\text{L}^{-1}$ of resorcinol pharmaceuticals over time. The anther considers the synchronization of system outputs a new method in the NAG-4SX3-3D analyzer.



Scheme 2. Proposed reaction for resorcinol- $K_2Cr_2O_7$ system

Result and Discussion

The flow injection manifold system (Figure 1a) was used to investigate chemical and physical factors to determine the circumstances that would yield the reaction product, yellowish-green species, with the highest repeatability and sensitivity. The most straightforward strategy to optimize these variables was to keep them all constant while modifying them one by one.

Chemical variables

Effect of variable concentration of potassium dichromate

The measurements were carried out under the following conditions: A series of potassium dichromate solutions were generated by diluting the stock solution with distilled water to obtain concentrations ranging from 10 to 150 mmol.L⁻¹. Each line was measured three times with a reagent concentration of 15 mmol.L⁻¹, a sample volume of 115 μL, an open valve mode, and a flow rate of 2.8 mL.min⁻¹ for the carrier

stream (distilled water) and reagent. Figure 1a reveals the response profile for this investigation which shows that the energy transducer response fluctuates with potassium dichromate concentration when using the NAG-4SX3-3D analyzer.

It was noticed that an increase in the response of the colored species with an increase of potassium dichromate concentration up 100 mmol.L⁻¹, more than 100 mmol.L⁻¹ led to broadening in high peak maxima and increase the peak base width (Δt_B), this due to increase the intensity of colored species which play as an internal filter in front of detector that prevents remaining light after absorption process from passes to solar cell. Therefore, 100 mmol.L⁻¹ of potassium dichromate was selected as an optimum concentration in the following studies to give a maximum peak height and sharpness. The obtained result was tabulated in Table 1a, while Figure 1b and Table 1b demonstrate the segmentation pattern for selecting the optimum segment of Res. Systems, segment S₃ (i.e., 70-150 mmol.L⁻¹) for the resorcinol-K₂Cr₂O₇ system.

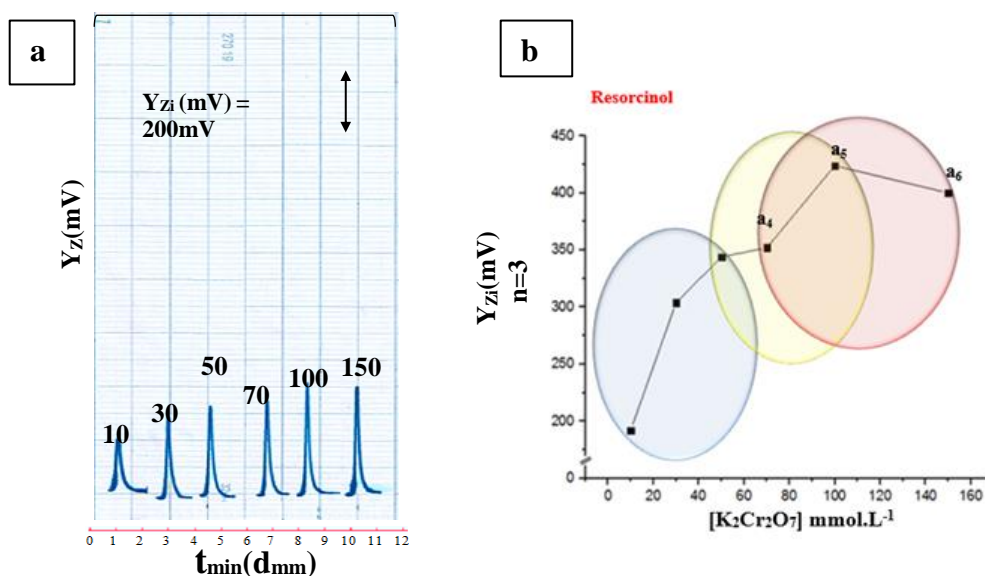


Figure 1. a) Response profile of potassium dichromate concentrations, b) Output of (S/N) energy transducer response, and three data points as one segment with optimum choice

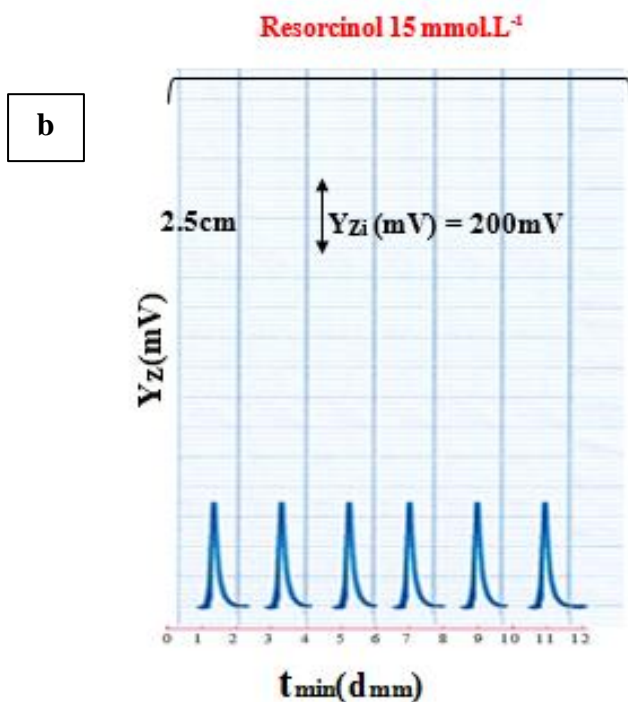
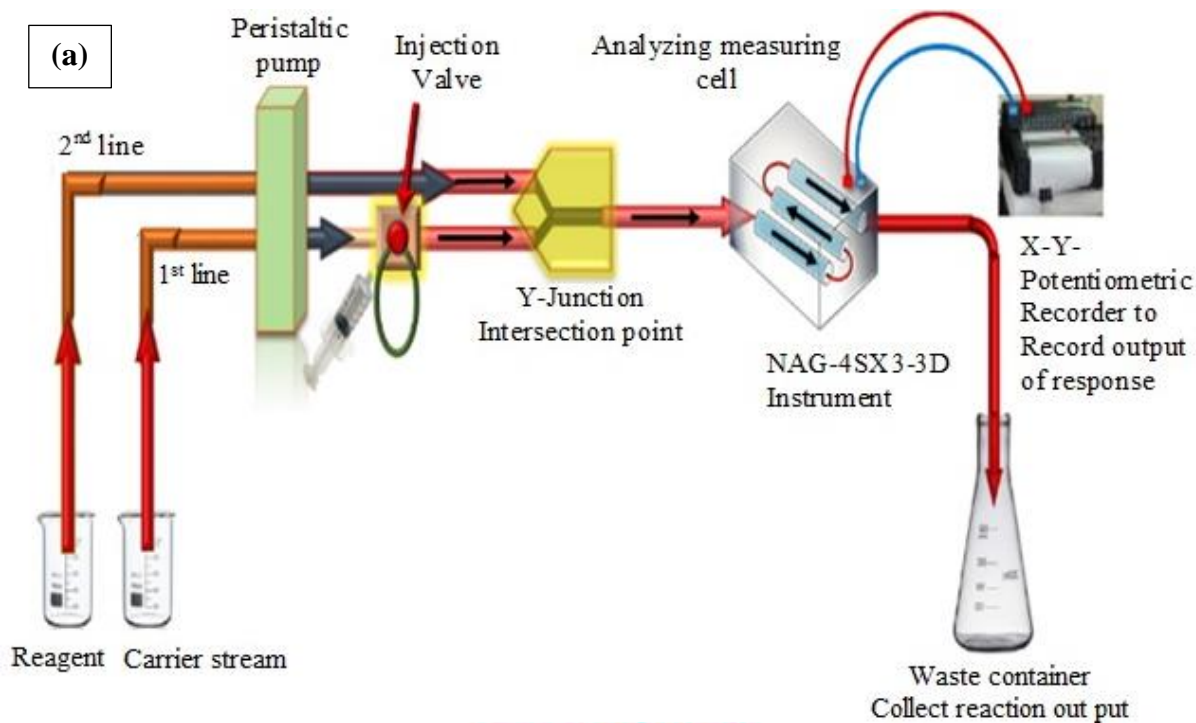


Figure 2. a) Diagram of manifold used for assessment NAG-4SX3-3D via reaction of resorcinol 15 mmol.L^{-1} with Potassium dichromate 50 mmol.L^{-1} to form yellowish green colored species. b) Profile of preliminary repeated experiments for assessment NAG-4SX3-3D instrument via reaction resorcinol with potassium dichromate to form yellowish species

Table 1. a) Effect of potassium dichromate concentration on precipitate formation of resorcinol, b) segmentation pattern slop-intercept with selection optimum segment for res-potassium dichromate system

| A | | | | | |
|--|---|-----------------|--|----------------------------|--------|
| [K ₂ Cr ₂ O ₇] mmol.L ⁻¹ | \bar{Y}_{zi} (mV) average (n=3) | RSD% | Confidence interval at 95% \bar{Y}_{zi} (mV)±t SEM | | |
| 10 | 192 | 0.59 | 192±2.807 | | |
| 30 | 304 | 0.40 | 304±3.056 | | |
| 50 | 344 | 0.40 | 344±3.428 | | |
| 70 | 352 | 0.35 | 352±3.080 | | |
| 100 | 424 | 0.43 | 424±4.497 | | |
| 150 | 400 | 0.58 | 400±4.764 | | |
| B | | | | | |
| Segment | [K ₂ Cr ₂ O ₇] range mmol.L ⁻¹ | Intercept mV | Slope mV/mmol.L ⁻¹ | correlation coefficient | Angle |
| S ₁ | 10-50 | 166.00 | 3.80 | 0.965 | 75.256 |
| S ₂ | 50-100 | 251.37 | 1.66 | 0.950 | 58.983 |
| S ₃ | 70-150 | 339.76 | 0.49 | 0.540 | 26.095 |

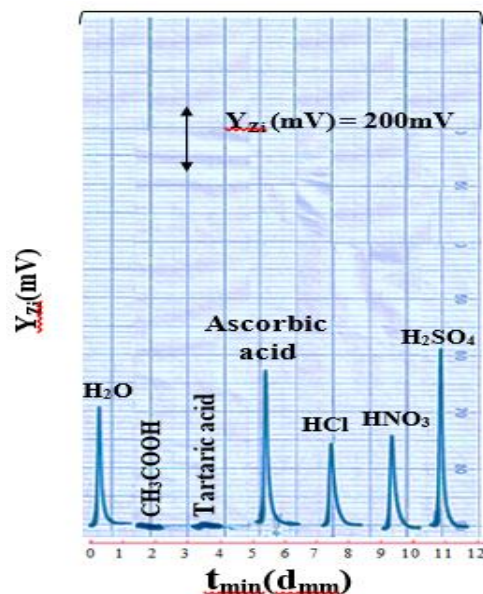
Effect of various medium

Using certain resorcinol system conditions, resorcinol 15 mmol.L⁻¹-K₂Cr₂O₇, 100 mmol.L⁻¹, and a 115 µL sample volume, 2.8 mL/min⁻¹ was the flow rate. The impact of various solutions was examined using a carrier stream. In addition to the aqueous medium, (CH₃COOH, Tartaric acid, Ascorbic acid, HCl, HNO₃, H₂SO₄, KCl, CH₃COONH₄) with a 0.4 mmol.L⁻¹ concentration. [Figure 3](#) shows that the investigated media generate a reduction in S/N-response. This might be due to a rise in agglomeration or the growth in aggregate density and compactness with one another, which leads to an increase in S/N response due to the effect of tiny solid particulate formation that causes a decrease in inter-spatial distances and increases incident light attenuation, this results in an increase in incident light intensity because there will be more empty spaces in between agglomerates of particulate except H₂SO₄. In this research study, H₂SO₄ medium was chosen as the best carrier stream for

resorcinol because it was suited for sensitivity and yielded a greater reaction. The acquired findings are summarized in [Table 2](#).

Effect of H₂SO₄ concentration

A variety of solutions ranging from 0.1 to 0.5 mmol.L⁻¹ were produced. With a sample volume of 115 µL, a flow rate of 2.8 mL.min⁻¹, an open valve mode, and a reagent concentration (K₂Cr₂O₇) of 100 mmol.L⁻¹, an initial concentration of resorcinol of 15 mmol.L⁻¹ was obtained. Each experiment was repeated three times, resulting in a rise in incident light attenuation as the concentration of H₂SO₄ increased. This was due to the shape of small-sized particulates, particularly if they were in the form of a nucleus, which accumulated in their packed blocked form, aiding in agglomeration. This will increase incident light attenuation of more than 0.5 mmol.L⁻¹ and an increase in small size solubility. The best carrier stream was 0.5 mmol.L⁻¹ of H₂SO₄. [Table 3](#) shows the results.

Figure 3. Effect of medium on response profile**Table 2.** Effect of different medium

| Type of medium 0.4 mmol.L ⁻¹ | \bar{Y}_{zi} (mV) average (n=3) | RSD% | Confidence interval at 95% \bar{Y}_{zi} (mV) ± t SEM |
|--|--------------------------------------|-------|---|
| H ₂ O | 424 | 0.41 | 424±4.298 |
| CH ₃ COOH | 0 | 0 | 0±0 |
| Tartaric acid | 8 | 12.25 | 8±2.435 |
| Ascorbic acid | 504 | 0.31 | 504±3.900 |
| HCl | 256 | 0.75 | 256±4.770 |
| HNO ₃ | 320 | 0.63 | 320±5.043 |
| H ₂ SO ₄ | 624 | 0.34 | 624±5.217 |

Table 3. Effect of variation H₂SO₄ concentration precipitation of resorcinol

| [H ₂ SO ₄] mmol.L ⁻¹ | \bar{Y}_{zi} (mV) average (n=3) | RSD% | Confidence interval at 95% \bar{Y}_{zi} (mV) ± t SEM |
|--|--------------------------------------|------|---|
| 0.1 | 120 | 0.86 | 120±2.559 |
| 0.2 | 264 | 0.75 | 264±4.919 |
| 0.3 | 448 | 0.44 | 448±4.894 |
| 0.4 | 624 | 0.32 | 624±4.993 |
| 0.5 | 800 | 0.26 | 800±5.093 |

Physical variables

Flow rate

An optimal concentration of Res. (15 mmol.L⁻¹), K₂Cr₂O₇ (100 mmol.L⁻¹), and H₂SO₄ (0.5 mmol.L⁻¹) were used with a sample volume of 115 μL. The flow rate varied from 1 mL.min⁻¹ to 4 mL.min⁻¹. Table 4 summarizes the results collected. At low flow rates, the response time

Δt_B was higher, as was the deformation of the top maximum peak response. This is due to an increase in the factor of dispersion. There was a drop in peak height when the flow rate was more than 2 mL.min⁻¹, which might be attributed to dispersion and dilution, resulting in an uneven response profile. As a result, the optimal flow rate for the resorcinol system was determined to be 2 mL.min⁻¹.

Sample volume

Variation sample volumes (82, 115, 139, 141, 175, and 281 μL) with open valve mode were evaluated with an appropriate flow rate of $2 \text{ mL}\cdot\text{min}^{-1}$ for the carrier stream and reagent. The concentration of resorcinol used was $15 \text{ mmol}\cdot\text{L}^{-1}$. An increase in sample volume increased response height without affecting the response profile (Table 5). Above 175 μL , the peak maximum widened, the base width (Δt_{B}) increased, or the peak height decreased. The ideal volume for resorcinol to provide a better response profile was 175 μL , as shown in Figure 4.

Effect of reaction loop lengths

Coil lengths ranging from 0 to 30 cm were investigated. These lengths contain a volume of 0–942 μL directly linked after the Y-junction in the flow system Figure 5. The Res. ($15 \text{ mmol}\cdot\text{L}^{-1}$)-100 $\text{mmol}\cdot\text{L}^{-1}$ $\text{K}_2\text{Cr}_2\text{O}_4$ -0.5 $\text{mmol}\cdot\text{L}^{-1}$ H_2SO_4 system was utilized with a sample volume of 175 μL . The effect of reaction coil length on sensitivity as measured by the S/N energy transducer response it was determined that raising the reaction coil caused the response height to increase without changing the response profile. A larger volume ($>785 \mu\text{L}$) resulted in a widening of the peak height and an increase in the base width (Δt_{B}), most likely because of the continuously extended time duration of color species in front of the detector.

Table 4. Effect of Variation flow rate on precipitation formation of resorcinol

| Pump speed Flow rate for each line | Flow rate $\text{mL}\cdot\text{min}^{-1}$ | $\bar{Y}_{\text{zi}}(\text{mV})$ average (n=3) | RSD% | Confidence interval at 95% $\bar{Y}_{\text{zi}}(\text{mV}) \pm t_{\text{SEM}}$ | Δt_{sec} | V_{add} (mL) at flow rate | C ($\text{mmol}\cdot\text{L}^{-1}$) | D.F | t_{sec} |
|---------------------------------------|--|--|------|---|-------------------------|---------------------------------------|--|---------|------------------|
| 5 | 1.0 | 1896 | 0.12 | 1896 ± 5.764 | 162 | 5.515 | 0.3128 | 47.9565 | 90 |
| 10 | 1.5 | 1976 | 0.12 | 1976 ± 6.012 | 114 | 5.815 | 0.2966 | 50.5655 | 54 |
| 15 | 2.0 | 1976 | 0.10 | 1976 ± 5.093 | 54 | 3.715 | 0.4643 | 32.3043 | 30 |
| 20 | 2.5 | 1900 | 0.10 | 1900 ± 4.919 | 60 | 5.115 | 0.3372 | 44.4783 | 24 |
| 25 | 2.8 | 800 | 0.25 | 800 ± 5.043 | 90 | 8.515 | 0.2026 | 74.0435 | 36 |
| 30 | 3.0 | 720 | 0.30 | 720 ± 5.391 | 60 | 6.115 | 0.2821 | 53.1739 | 18 |
| 35 | 3.5 | 600 | 0.37 | 600 ± 5.540 | 54 | 6.415 | 0.2689 | 55.7826 | 12 |
| 40 | 4.0 | 480 | 0.50 | 480 ± 6.012 | 42 | 5.715 | 0.3018 | 49.6957 | 12 |

Table 5. Effect of variation sample volume on precipitation formation of resorcinol

| Length of sample segment cm r=0.5 | Sample volume μL | $\bar{Y}_{\text{zi}}(\text{mV})$ average (n=3) | RSD% | Confidence interval at 95% $\bar{Y}_{\text{zi}}(\text{mV}) \pm t_{\text{SEM}}$ | Δt_{sec} | V_{add} (mL) at flow rate | C ($\text{mmol}\cdot\text{L}^{-1}$) | D.F | t_{sec} |
|--------------------------------------|--------------------------------|--|------|---|-------------------------|---------------------------------------|--|---------|------------------|
| 10.4 | 82 | 304 | 0.77 | 304 ± 5.813 | 72 | 4.882 | 0.252 | 59.5366 | 30 |
| 14.6 | 115 | 1000 | 0.23 | 1000 ± 5.739 | 90 | 6.115 | 0.282 | 53.1739 | 36 |
| 17.7 | 139 | 1976 | 0.10 | 1976 ± 4.993 | 90 | 6.139 | 0.340 | 44.1655 | 36 |
| 18 | 141 | 1980 | 0.10 | 1980 ± 4.919 | 90 | 6.141 | 0.344 | 43.5532 | 36 |
| 22.3 | 175 | 2020 | 0.10 | 2020 ± 4.894 | 90 | 6.175 | 0.425 | 35.2857 | 36 |
| 35.8 | 281 | 2520 | 0.13 | 2520 ± 7.974 | 78 | 5.481 | 0.769 | 19.5053 | 36 |

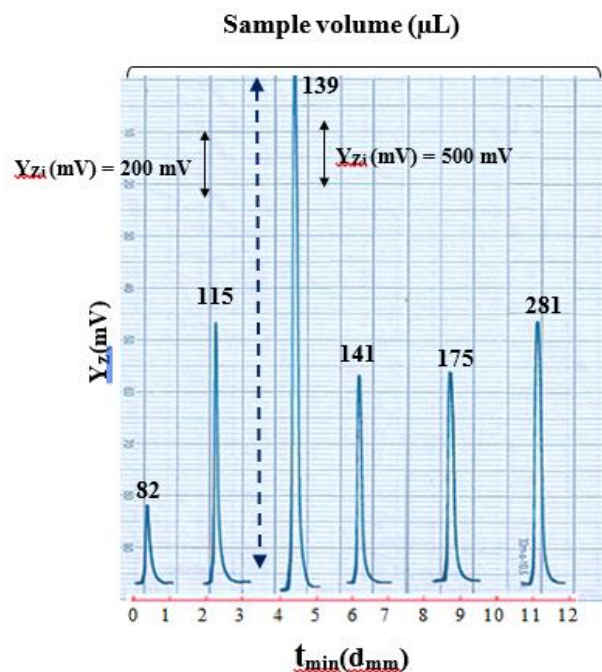


Figure 4. Response of varies sample volume on energy transducer response

The Y-junction plays a critical role in the reaction's reactant mixing. The Y-junction was directly linked before the measurement cell in the flow system. Its influence on the response profile was investigated by varying the Y-junction at different parameters (Figure 6). The optimal concentration of Res. ($15 \text{ mmol}\cdot\text{L}^{-1}$) was utilized with a sample volume of $175 \mu\text{L}$ and a flow rate of $2 \text{ mL}\cdot\text{min}^{-1}$ for both the carrier stream and the reagent. Figure 6 depicts the whole profile of the Y-junction (meeting zone) impact of the S/N transducer energy response that was acquired. To investigate the influence on agglomeration, regulation, and regular distribution of particulates prior to the flow tube's entry, a variety of volume mixing

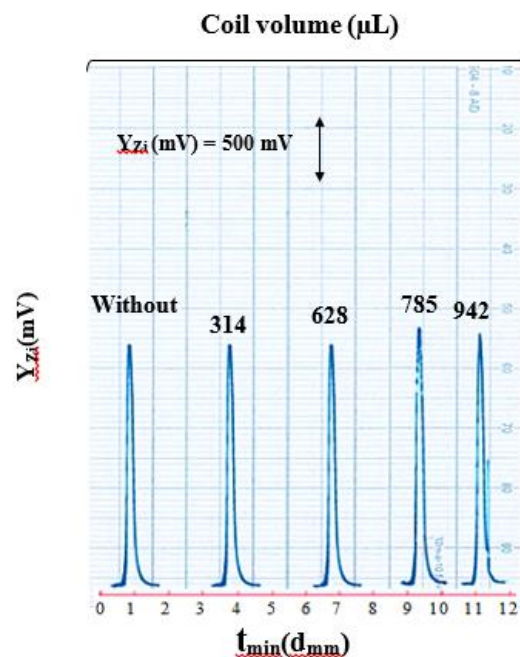


Figure 5. Response profile of coil volume on energy transducer response for the assessment of NAG-4SX3-3D via formation of yellowish green species

chambers and an intersecting point in a larger diameter were used. However, particle scattering and dispersion and rising inter-spatial distances create a decrease in the capacity to prevent incident light from raising the height of the response measurement of the energy transducer Table 6. As a result, it was thought that removing the premix chamber or the crossing point at a higher tube diameter might be accomplished by using a manifold unit with 3 mm (I.D) entrances and a 3 mm (I.D) output. These indicate that the best Y-junction for mixing reactants and formation of precipitate particles in a sulfuric acid medium is $21.2 \mu\text{L}$.

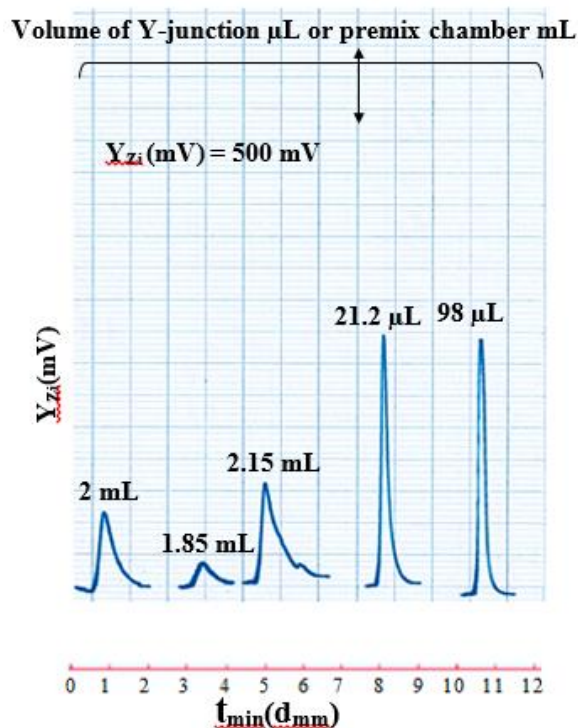


Figure 6. Response profile for assessing NAG-4SX3-3D instrument via formation of colored species of resorcinol

Table 6. Data set point obtained for Volume of Y-junction & premix chamber in the determination procedure of resorcinol

| Type of Y-junction | Volume $\pi r^2 h$ | \bar{Y}_{zi} (mV) average (n=3) | t_{sec} | Volume mL At junction point | C (mm/L) DF | |
|-----------------------------|--------------------|-----------------------------------|-----------|-----------------------------|-------------|---------|
| Intersection junction point | 3 mm (ID) | 21.2 μ L | 2020 | 34 | 2.4629 | 1.0658 |
| | 3 mm (thickness) | | | | | 14.0735 |
| | 5 mm (ID) | 98.00 μ L | 784 | 34.5 | 2.5730 | 1.0202 |
| | 5 mm (thickness) | | | | | 14.7029 |
| Premix chamber | 14 mm (ID) | 1.85 mL | 80 | 35 | 4.3583 | 0.6023 |
| | 12 mm (thickness) | | | | | 24.9048 |
| | 14 mm (ID) | 2.00 mL | 248 | 36 | 4.5750 | 0.5738 |
| | 13 mm (thickness) | | | | | 26.1429 |
| | 14 mm (ID) | 2.15 mL | 312 | 36.5 | 4.7583 | 0.5517 |
| | 14 mm (thickness) | | | | | 27.1905 |

Determining the linear dynamic range for the variation of resorcinol on the S/N energy transducer response using a scatter plot

Physical and chemical variables were adjusted to their optimum values in the preceding section (Res- $K_2Cr_2O_7$ (100 mmol.L⁻¹)- H_2SO_4 (0.5 n mmol.L⁻¹) system, 175 μ L sample

volume, no delay reaction coil, and 2.5 mL.min⁻¹ flow rate for both carrier and reagent lines). For resorcinol, various organic compound solutions (0.05–50 mmol.L⁻¹) were created. Each measurement was taken three times. The average peak height (mV) of the transducer's energy response was plotted versus the concentration of the organic component. A

straight line graph (Figure 7a, b, c) was observed from 0.05 to 32 mmol.L⁻¹ of resorcinol. Above 32 mmol.L⁻¹, the correlation coefficient value will drop, and linearity will be compromised. This is most definitely attributable to an increase in colored species in front of the detector, which might be related to light attenuation. The freshly established approach for determining resorcinol was compared to an existing reference method [13]. Specifically, the spectrophotometric method shown in Figures 8a and b, and Table 7 summarize the result obtained.

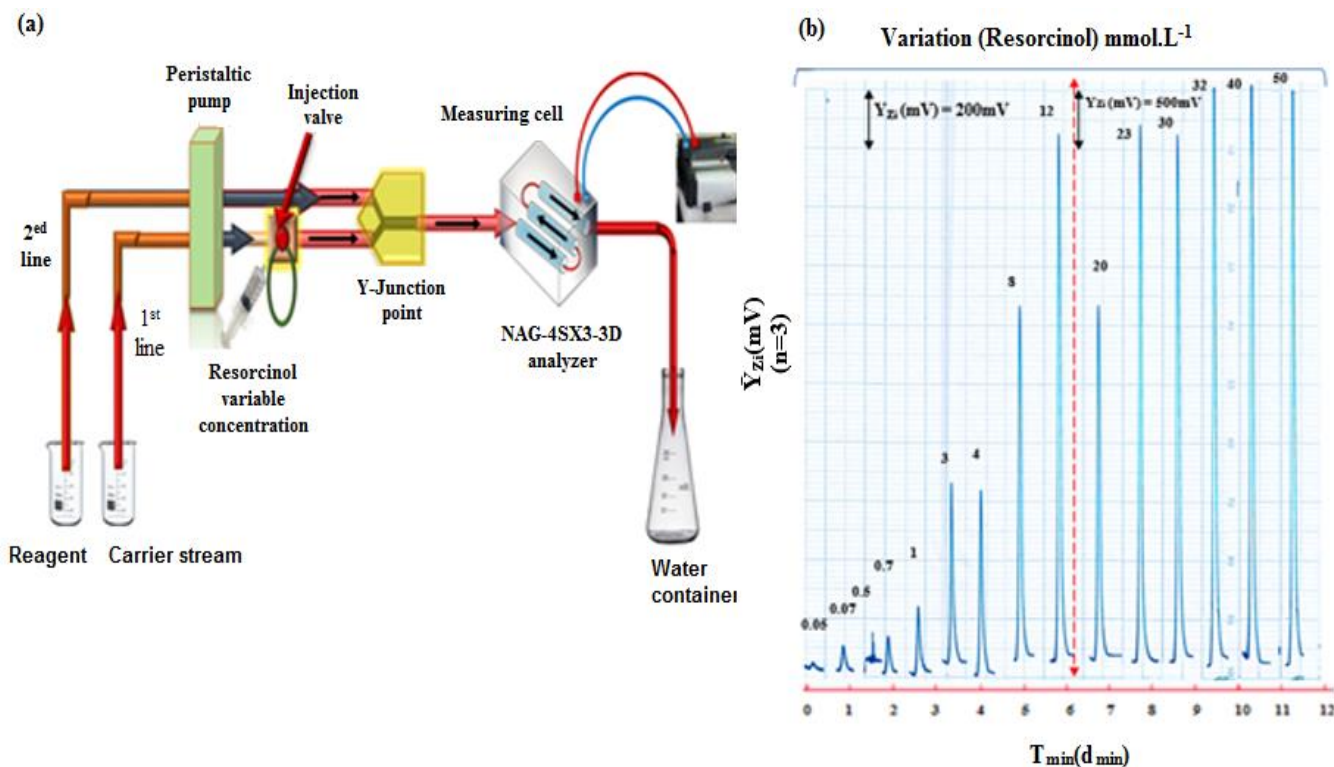
Limit of detection (LOD)

The limit of detection of resorcinol was calculated using three different methods, as tabulated in Table 8.

Repeatability

The measurements of two concentrations of catechol obtained across the whole test method in terms of precision summarize in Figure 9 and Table 9. Each measurement was done six times. The relative standard deviation was less than 0.2%, as shown in Figure 9 depicts a response profile for the concentrations applied.

Under the established optimum conditions (Res. (variable concentration)-K₂Cr₂O₇ (100 mmol.L⁻¹ system, with 175 L sample volume, 2.5 mL.min⁻¹ flow rate, and 21.2 μL Y junction point) the detailed comparison was made against the Uv-spectrophotometric (λ_{\max} =273 nm) (for resorcinol) at the constant concentration used through the dynamic calibration range.



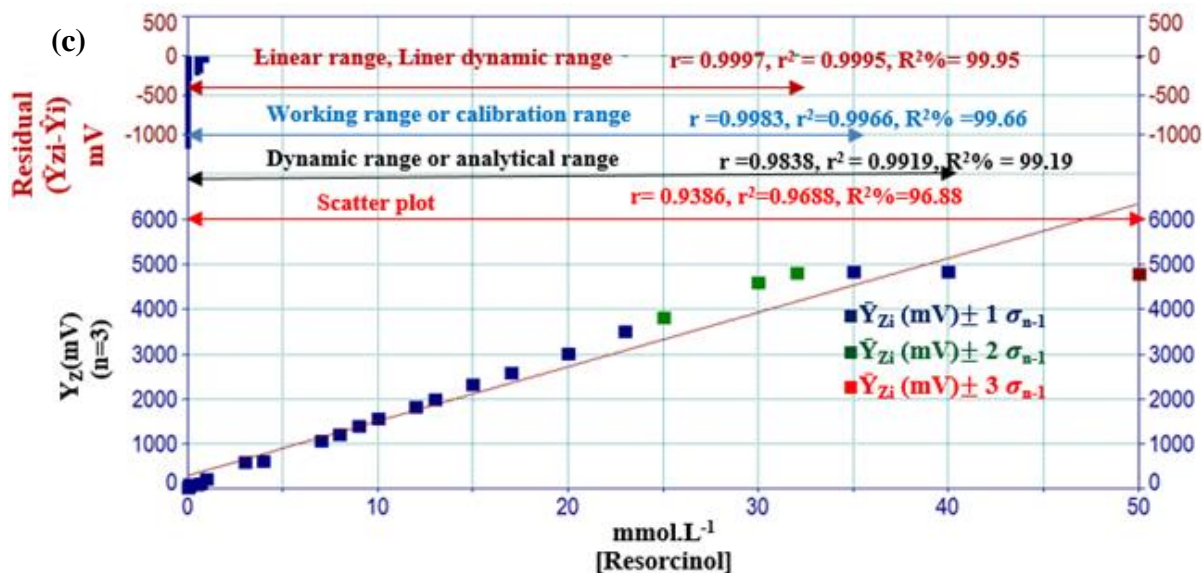


Figure 7. a) Flow gram system used for the determination of resorcinol, b) Some of the profiles versus time, potentiometric scanning speed 1 cm.min⁻¹, c) Different range for the effect of resorcinol concentration on attenuation of incident light using NAG-4SX3-3D analyzer for scatter plot range (0.005-2.5) mmol.L⁻¹ for n=16

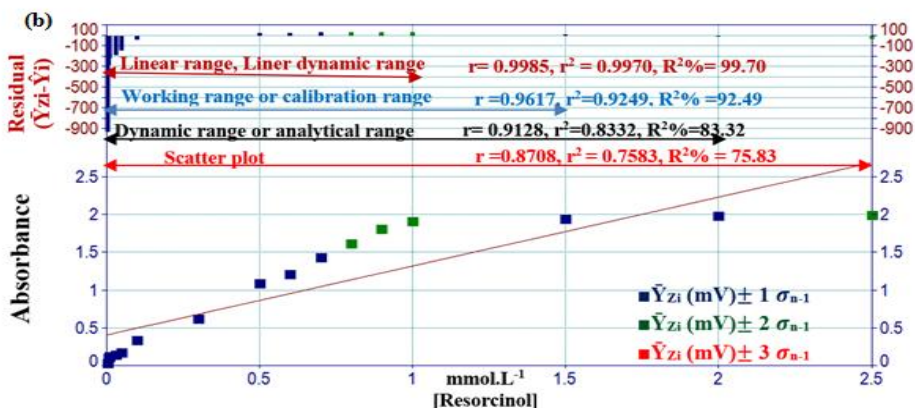
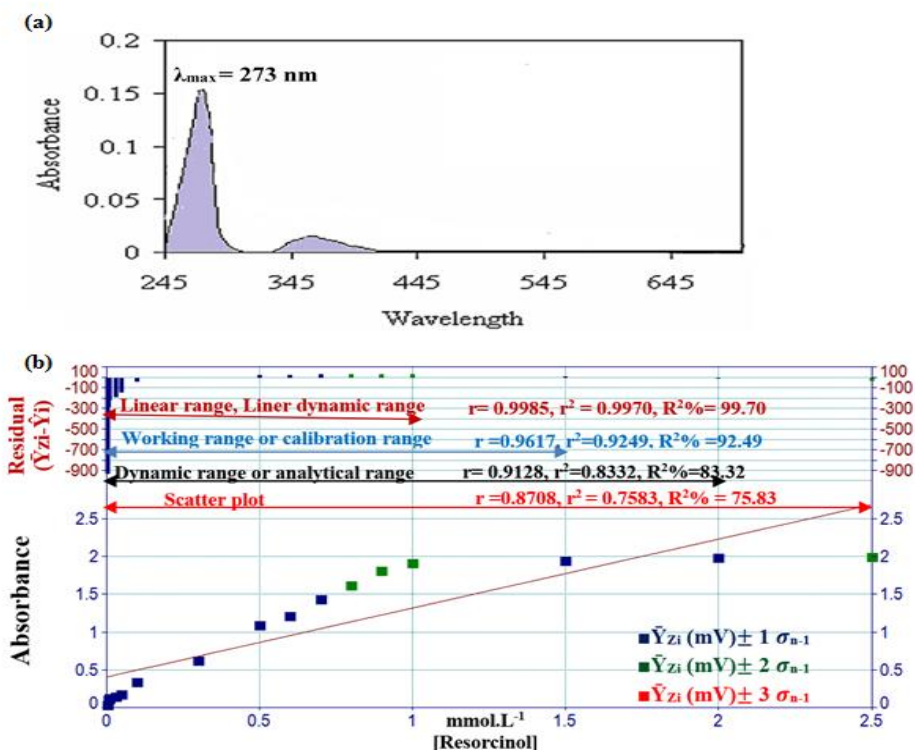


Figure 8. a) Uv-spectrum of resorcinol in $\lambda_{max}=273$ nm, b) The scatter for resorcinol using a classical method at $\lambda_{max}=273$ nm

Table 7. Summary of results for linear regression for the variation of (S/N) energy transducer response with resorcinol concentration using first-degree equation of the form $\hat{Y}=a+ b x$ at optimum conditions

| Type of mode | Range of [Fe (II)] ion mmol.L ⁻¹ (n) | $\hat{Y}_{Zi}=a \pm S_a t+b(\Delta y / \Delta x_{\text{mmol/L}}) \pm S_b t$ [Fe (II)] mmol.L ⁻¹ at confidence level 95%, n-2 | r, r ² , R ² % | t _{tab} at 95%, n-2 | Calculated t-value $t_{\text{cal}}=r/\sqrt{n-2} / \sqrt{1-r^2}$ |
|---|---|---|--------------------------------------|------------------------------|--|
| Developed method using NAG-4SX3-3D analyzer UV- Spectrophotometer at $\lambda_{\text{max}}=273\text{nm}$. | | | | | |
| Linear range or linear dynamic range | 0.05-32 (21) | 52.6162±24.5164+149.9786±1.6518 [Res.] mmol.L ⁻¹ | 0.9997, 0.9995, 99.95 | 2.093<<190.031 | |
| Working range or calibration range | 0.005-1 (13) | 0.0946±0.0361+1.8807±0.0680 [Res.] mmol.L ⁻¹ | 0.9985, 0.9970, 99.70 | 2.2010<<60.8102 | |
| Dynamic range or analytical range | 0.05-35 (22) | 80.4651±64.9562+145.8924±3.9832 [Res.] mmol.L ⁻¹ | 0.9983, 0.9966, 99.66 | 2.086<<76.405 | |
| Dynamic range or analytical range | 0.005-1.5 (14) | 0.1877±0.1780+1.5302±0.2743 [Res.] mmol.L ⁻¹ | 0.9617, 0.9249, 92.49 | 2.1788<<12.158 | |
| Dynamic range or analytical range | 0.05-40 (23) | 146.1495±144.1704+137.4224±8.0101 [Res.] mmol.L ⁻¹ | 0.9838, 0.9919, 99.19 | 2.080<<35.6846 | |
| Scatter plot | 0.005-2 (15) | 0.3058±0.2554+1.1727±0.3143 [Res.] mmol.L ⁻¹ | 0.9128, 0.8332, 83.32 | 2.160<<8.059 | |
| Scatter plot | 0.05-50 (24) | 278.0270+120.7758±13.6541 [Res.] mmol.L ⁻¹ | 0.9386, 0.9688, 96.88 | 2.0739<<18.344 | |
| Scatter plot | 0.005-2.5 (16) | 0.4089±0.2958+0.9094±0.2943 [Res.] mmol.L ⁻¹ | 0.8708, 0.7583, 75.83 | 2.145<<6.628 | |

n: no. of measurement, \hat{Y}_{Zi} (mV); estimated response (n=3) in mV for developed method and \hat{Y}_{Zi} = estimated value without uniting for a spectrophotometric method or in NTU for turbidimetric method, r: correlation coefficient, r²: coefficient of determination, R²% (percentage capital R- squared): explained variation as a percentage/total variation and $t_{\text{tab}}= t_{0.05/2}$, n-2, the volume of measuring cell 1 mL for UV-Sp. and 10 mL for turbidimetric

Table 8. Detection Limit of Resorcinol using 175 μL as an injection sample and optimum parameters using Res (15 mmol.L⁻¹)-[K₂Cr₂O₇] (100 mmol.L⁻¹)- H₂SO₄ (0.5 mmol.L⁻¹) system

| Practically based on the gradual dilution for the minimum concentration in scatter plot | | | | |
|---|---|---|---|--|
| Newly developed method (0.0025) mmo.L ⁻¹ | Classical method spectrophotometric method (0.001) mmol.L ⁻¹ | Theoretical based on the value of slope $x=3S_B/\text{slope}$ | Theoretical based on the linear equation $\hat{Y}=Y_b + 3S_b$ | Limit of quantitative L.O. Q $\hat{Y}=Y_b+10S_b$ |
| 48.1687 ng/sample | 0.1101 $\mu\text{g}/\text{sample}$ | 0.2235 $\mu\text{g}/\text{sample}$ | 13.9307 $\mu\text{g}/\text{sample}$ | 46.4356 $\mu\text{g}/\text{sample}$ |

Table 9. Repeatability of resorcinol at optimum parameters with 175 μL sample volume

| Concentration of resorcinol mmol.L ⁻¹ | \bar{Y}_{Zi} (mV) average responses (n=6) | RSD% | Confidence interval at 95% $\bar{Y}_{Zi}(\text{mV}) \pm t_{0.05/2} \sigma_{n-1}/\sqrt{n}$ |
|--|---|-------|--|
| 0.7 | 120 | 0.290 | 120±0.3496 |
| 23 | 3500 | 0.082 | 3500±1.3786 |

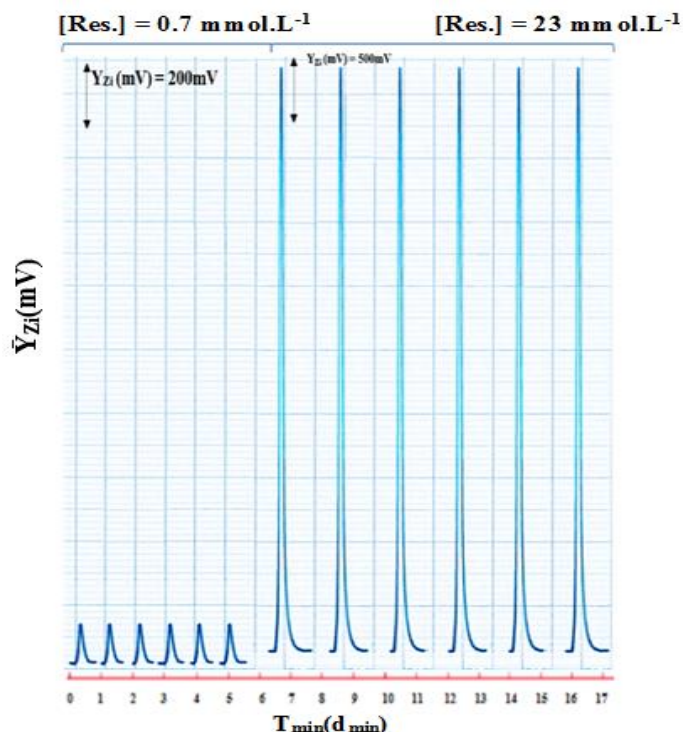


Figure 9. $Y_{Zi}(mV) - t_{(min)}(d_{min})$ profile of seven successive measurements with repeatability of profile for 0.7 mmol.L^{-1} and 23 mmol.L^{-1} concentration of [resorcinol] using $K_2Cr_2O_7$ (100 mmol.L^{-1})- H_2SO_4 (70 mmol.L^{-1}), using $175 \mu\text{L}$ as injection of sample loop and 2 mL.min^{-1} flow rate for each line. Also, high measurement repeatability at six high sensitivity of using $25 \text{ mm} \rightarrow 500 \text{ mV}$

Comparison between reference methods already used with newly developed method using the NAG 4SX3-3D instrument, the comparison based on the sensitivity.

Table 10 contains an overview of the study's findings. Figure 10a, b illustrates a plot of two separate Y-axes at constant concentrations of resorcinol produced by calibration graph creation and a plot of Uv-spectrophotometric absorbance as a dependent variable against Uv-spectrophotometric absorbance NAG-4SX3-3D

analyzer response for the same concentration (ranging from $0.05\text{-}1 \text{ mmol.L}^{-1}$). The slope value using the NAG-4SX3-3D analyzer (172.2043) is $>45^\circ$ (89.38°) more than using the classical method of Uv-spectrophotometric (1.8495) (Table 10), indicating that there is a significant difference between the two methods, i.e., the developed method has 93 times ($172.2043/1.8495=93.109$) more sensitivity than the traditional method.

Table 10. Summary of results for different methods using one molecule (Resorcinol molecule)

| [Res] mmol/L Independed variable | Resorcinol molecule | | | | | |
|-------------------------------------|---|----------------|--|--|--------|---|
| | Measurements expressed as an average of responses (n=3) | | | | | \bar{y}_i developed Vs \bar{y}_{iAbs} . |
| | Developed method NAG-4SX3-3D analyzer | | Abs. at $\lambda_{max}=273 \text{ nm}$ | | | |
| $\bar{y}_i(mV)$ | $\hat{y}_i(mV)$ | \bar{y}_iAbs | \hat{y}_iAbs | $\hat{y}_{i(devl \text{ method} - Abs)}$ | | |
| 0.05 | 24 | 48.90 | 0.181 | 0.210 | 46.403 | |
| 0.1 | 98 | 57.51 | 0.34 | 0.303 | 61.171 | |
| 0.3 | 96 | 91.95 | 0.62 | 0.673 | 87.177 | |

| | | | | | |
|---|---|--|--|-------|----------------------|
| 0.5 | 104 | 126.39 | 1.093 | 1.042 | 131.109 |
| 0.6 | 135 | 134.61 | 1.21 | 1.227 | 141.976 |
| 0.7 | 156 | 160.83 | 1.43 | 1.412 | 162.410 |
| 0.8 | 178 | 178.05 | 1.619 | 1.600 | 179.964 |
| 0.9 | 200 | 195.27 | 1.81 | 1.782 | 197.704 |
| 1.0 | 224 | 212.49 | 1.911 | 1.967 | 207.085 |
| Linear regression at confidence level 95%, $n-2 \hat{y}_i = a \pm S_a t + b \pm S_b t$ [Res] mmol/L $r, r^2, R^2\%$ | $40.2876 \pm 32.497 + 172.2043 \pm 51.009$ [Res] mmol/l | $0.1177 \pm 0.066 + 1.8495 \pm 0.104$ [Res] mmol/l | $29.5921 \pm 35.436 + 92.8795 \pm 27.647$ [Res] mmol/l | | 7.647 [Res] mmol/l |
| | 0.9492, 0.9010, 90.10 | 0.9980, 0.9461, 99.61 | 0.9488, 0.9002, 90.02, 89.38° | | |

X: Esorcinol molecule, \hat{y}_i : in mV for developed method, without uniting for UV-Sp method., r: correlation coefficient, r^2 : coefficient of determination, $R^2\%$ (percentage capital R- squared): explained variation as a percentage/total variation, UV-Sp.: UV -Spectrophotometric method, using a volume of the cell (quartz) 1 mL in UV-Spectrophotometric method

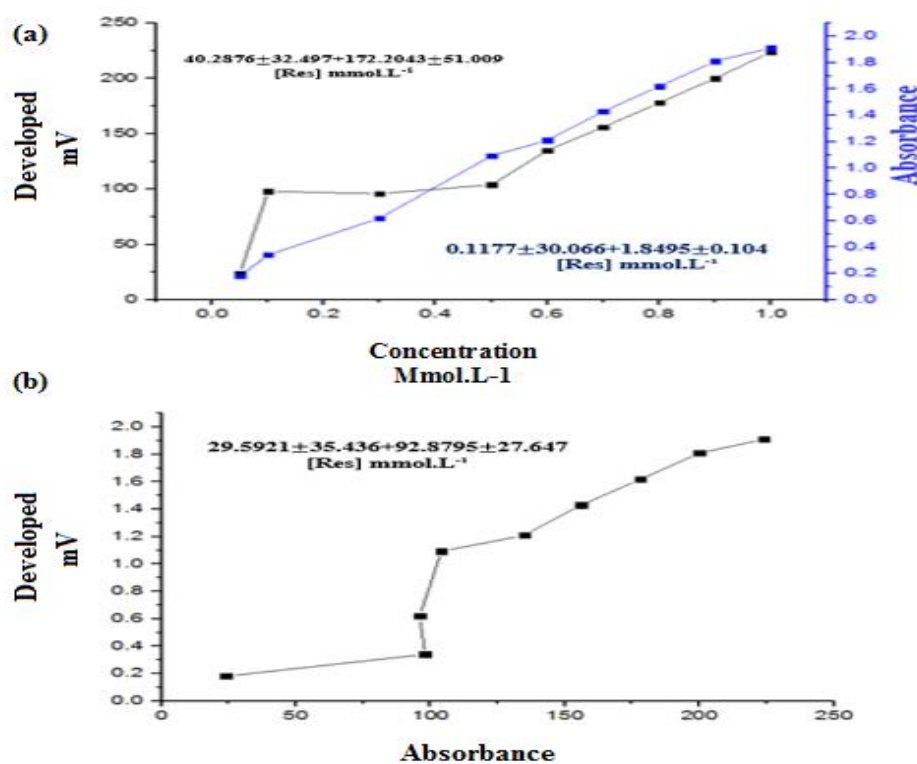


Figure 10. a) Energy transducer response expressed as an average peak heights (mV) using NAG-4SX3-3D analyzer and Uv spectrophotometric method at $\lambda_{max}=273nm$. b) Y predicted (\hat{Y}_i) using two methods NAG4SX3-3D Analyser (mV) and classical method Uv-spectrophotometry

Conclusions

The suggested approach is less costly than standard methods in apparatus and reagents. The NAG-4SX3-3D analyzer was employed in this investigation to produce a more accurate and faster result. The repetition RSD percent

($n=6$) was much lower than 0.3%, indicating that the proposed approach is precise enough. This approach may also be used to identify resorcinol, and it has the added feature of being able to achieve high sensitivity without using heat or extraction. The statistical analysis

results were identical to those obtained using the conventional technique.

Disclosure Statement

No potential conflict of interest was reported by the authors.

Orcid

Sarah Faris Hameed  0000-0002-8700-6389

Reference

- [1]. Kamonwad N., Tharat B., Hirunsit P., Suthirakun S. *RSC Adv.*, 2020, **10**:28454 [[Crossref](#)], [[Google Scholar](#)], [[Publisher](#)]
- [2]. Kumawat P., Chanda J., Das S.K., Ghosal A., Gupta S.D., Mukhopadhyay R. *Polym Eng Sci.*, 2021, **61**:864 [[Crossref](#)], [[Google Scholar](#)], [[Publisher](#)]
- [3]. Senthil R.A., Selvi A., Arunachalam P., Amudha L.S., Madhavan J., Al-Mayouf A.M. *J Mater Sci.*, 2017, **28**:10081 [[Crossref](#)], [[Google Scholar](#)], [[Publisher](#)]
- [4]. Tokudome Y., Hoshi T., Mori S., Hijikuro I. *Cosmetics*, 2020, **7**:55 [[Crossref](#)], [[Google Scholar](#)], [[Publisher](#)]
- [5]. Vachiramon V., Kositkuljorn C., Leerunyakul K., Chanprapaph K. *J Cosmet Dermatol.*, 2021, **20**:987 [[Crossref](#)], [[Google Scholar](#)], [[Publisher](#)]
- [6]. Cheng B., Ren Y., Cao H., Chen J. *Eur. J. Med. Chem.*, 2020, **199**:112377 [[Crossref](#)], [[Google Scholar](#)], [[Publisher](#)]
- [7]. Topçu E. *Mater. Res. Bull.*, 2020, **121**:110629 [[Crossref](#)], [[Google Scholar](#)], [[Publisher](#)]
- [8]. Huang L., Cao Y., Diao D. *Sensors and Actuators B: Chemical*, 2020, **305**:127495 [[Crossref](#)], [[Google Scholar](#)], [[Publisher](#)]
- [9]. Manjunatha J.G. *Chemical Data Collections*, 2019, **25**:100331 [[Crossref](#)], [[Google Scholar](#)], [[Publisher](#)]

[10]. Körbahti B.K., Demirbüken P. *Frontiers in Chemistry*, 2017, **5**:75 [[Crossref](#)], [[Google Scholar](#)], [[Publisher](#)]

[11]. Yin D., Liu J., Bo X., Guo L. *Anal. Chim. Acta.*, 2019, **1093**:35 [[Crossref](#)], [[Google Scholar](#)], [[Publisher](#)]

[12]. Shakir I.M.A., Al-Awadie N.S.T. IRQ. PATENT. No. 6100. 2020, Novel Multiple Continuous Flow Cells (hydrophilic & hydrophobic) works as a Solo Flow cell with Summed S/N responses in NAG-4SX3-3 D.

[13]. Blanco S.E., Almandoz M.C., Ferretti F.H. *Spectrochim. Acta, Part A*, 2005, **93** [[Crossref](#)], [[Google Scholar](#)], [[Publisher](#)]

How to cite this manuscript: Nagham Shakir Turkie, Sarah Faris Hameed*, Continuous flow injection analysis via NAG-4SX3-3D analyzer utilized to determination of resorcinol. *Asian Journal of Green Chemistry*, 6(2) 2022, 129-144. DOI: 10.22034/ajgc.2022.2.3